Anomalous dynamical charges, phonons, and the origin of negative thermal expansion in $Y_2W_3O_{12}$

S. Sumithra,[1] U. V. Waghmare,[2] and A. M. Umarji[1]
[1]*Materials Research Centre, Indian Institute of Science, Bangalore 560 012, India*
[2]*Theoretical Sciences Unit, Jawaharlal Nehru Centre for Advanced Scientific Research, Jakkur, Bangalore 560 064, India*
(Received 9 January 2007; revised manuscript received 23 May 2007; published 16 July 2007)

We use a combination of classical model and first-principles density functional theory calculations to study lattice dynamics of $Y_2W_3O_{12}$ and identify phonons responsible for its negative thermal expansion (NTE). Born dynamical charges of various atoms are found to deviate anomalously from their nominal values. We find that the phonons with energy from 4 to 10 meV are the primary contributors to its NTE. These phonons involve rotations of the YO_6 octahedra and WO_4 tetrahedra in mutually opposite sense and collective translational atomic displacements, reflecting a strong mixing between acoustic and optic modes.

DOI: 10.1103/PhysRevB.76.024307 PACS number(s): 63.20.−e, 65.40.De, 78.30.−j

Most solids expand upon heating due to anharmonicity of the chemical bond[1] and the distance between the chemically bonded atoms generally increases. A new class of materials, discovered in 1996, is an exception to this rule and shrinks when heated.[2,3] These exotic materials [known as negative thermal expansion (NTE) materials] have generated considerable interest due to its broad range of possible applications ranging from optical mirrors to printed circuit boards. The phenomenon of NTE is attributed to the unique geometry of the crystal structure and unusual lattice dynamics. Crystal structure of these materials is characterized by corner shared MO_n polyhedra and often exhibits an open framework. A cooperative rocking motion of polyhedra *as rigid units*[4] can be a cause for the NTE. However, not all compounds with open framework structure exhibit NTE, and it is fundamentally interesting to understand the origin of NTE. In this present work, we investigate the phonon modes in greater depth and identify additional criteria for the NTE.

Negative thermal expansion was discovered in cubic ZrW_2O_8 (Ref. 2) which exhibits isotropic NTE from 0.3 to 1050 K. Experimental and theoretical simulation studies have been carried out to determine its phonon spectrum and related dynamics,[4–8] and understand its relevance to NTE. ZrW_2O_8 has a framework structure with corner shared ZrO_6 octahedra and WO_4 tetrahedra, and the NTE is attributed to the transverse thermal vibrations perpendicular to Zr-O-W linkages. Lattice dynamical calculations have established the presence of low-energy librational phonons extending down to zero energy called rigid unit modes (RUMs), which were shown to be partly responsible for the NTE in ZrW_2O_8.[4] Unusual dynamics of the low-energy phonons in ZrW_2O_8 was discovered in an infrared spectroscopic study recently,[9] showing a mixing of the librational (torsional) and translational motion.

Negative or low thermal expansion is known to occur in $PbTiO_3$ and also in some other AMO_3 oxides. It occurs due to anisotropic thermal expansion along the different crystallographic axes. Such an effect has also been shown in cordierite ($Mg_2Al_2Si_5O_{18}$), beta-eucryptite ($LiAlSO_4$), and NZP ($NaZr_2P_3O_{12}$).

Though NTE has been most studied in ZrW_2O_8, other oxides such as $A_2M_3O_{12}$ and AM_2O_7 (where A is an octahedral cation and M is a tetrahedral cation) also exhibit strong NTE behavior.[10,11] In $Y_2W_3O_{12}$ and ZrV_2O_7 oxides, NTE is attributed to transverse thermal vibrations perpendicular to Y-O-W and V-O-V linkages, respectively. NTE has been observed in $Y_2W_3O_{12}$, along all the crystallographic directions from 15 to 1373 K with an α_l of -7×10^{-6}/K.[12] It belongs to *Pnca* space group and its structure consists of corner shared YO_6 octahedra and WO_4 tetrahedra. All oxygen atoms in $Y_2W_3O_{12}$ have twofold coordination, in contrast to ZrW_2O_8 where one of the oxygens belonging to a WO_4 tetrahedron is coordinated with only one W atom.

To understand the cause for negative thermal expansion and probe the existence of soft modes, RUM calculations have been carried out for a variety of framework structure oxides.[13] The authors showed that the occurrence of RUMs in a structure does not necessarily correlate with its NTE property. In particular, RUMs were not found in $Y_2W_3O_{12}$, and it was found that transverse thermal vibrations are important for NTE.

Our earlier experimental work showed that $Y_2W_3O_{12}$ formed a trihydrate structure at room temperature and that NTE is observed only after a complete removal of water molecules.[14] To probe phonons relevant to its NTE using IR, Raman, or neutron scattering, one requires unhydrated sample at room temperature, which is difficult to prepare and maintain. Hence, we use here quantum mechanical simulations to determine Born dynamical charges which are relevant to IR spectra as well as indicators of soft vibrational modes,[15] and classical thermodynamic simulations to determine phonons and temperature dependent properties.

Born effective charge tensors $Z^*_{i\alpha\beta}$, which give electric dipole moment $\mu_\alpha = Z^*_{i\alpha\beta}u_{i\beta}$ associated with displacement u of an atom i in the β direction, are the coupling between phonons and IR radiation. These charges also give force on an atom: $F_{i\alpha} = Z^*_{i\alpha\beta}E_\beta$ due to applied electric field E. They are typically quite different from the nominal ionic charges in transition metal oxides and have been determined using first-principles pseudopotential based on density functional theory linear response calculations with ABINIT (Ref. 16) treating electric field perturbatively.[17]

Born effective charges are known to be anomalously large and indicators of soft modes in ferroelectric materials,[15,18]

TABLE I. Crystallographic positions at 293 K and eigenvalues of Born dynamical charge tensors for symmetry inequivalent atoms.

Atom	x	y	z	Z_1	Z_2	Z_3
Y	0.4686	0.3819	0.2482	5.25	4.85	4.53
W	0.25	0.0	0.4735	4.06	4.04	3.09
W	0.1146	0.3567	0.3916	4.21	3.88	3.34
O	0.0885	0.1400	0.0648	−4.08	−0.69	−0.58
O	0.1387	0.0643	0.3718	−4.18	−0.66	−0.59
O	0.0171	0.2656	0.3194	−4.37	−0.65	−0.61
O	0.3382	0.4181	0.0745	−3.66	−0.68	−0.67
O	0.0675	0.4677	0.3231	−3.68	−0.67	−0.63
O	0.2850	0.3376	0.3588	−3.83	−0.77	−0.60

which also exhibit NTE just below the ferroelectric transition temperature. Our results for these charges (see Table I) reveal that the effective charges of (i) Y are anomalously large, (ii) W are anomalously small, and more interestingly (iii) those of oxygen are large along the bonding direction and small along perpendicular directions (note that Y-O-W bond angles are about 150°–180°). While such an anisotropy is also observed in perovskites, magnitude of dynamical charges of oxygen and W being smaller than their nominal values is indeed unusual here. These results indicate a strong covalency or hybridization between the d states of transition metals and p states of oxygen. In octahedrally coordinated transition metal (TM) oxides, the effective charge of a TM is anomalously larger than its nominal value and its cause can be traced to the π-like interactions in the low-lying t_{2g} states of TM and p states of oxygen. For example, Z^* of octahedrally coordinated Y is about 3.7 in Y_2O_3 (Ref. 19) and of W is 12.5 in WO_3.[20] While the effective charge of Y in $Y_2W_3O_{12}$ is anomalously large, that of W is much smaller than its nominal value. A possible cause for this may be that the low-lying W states in the conduction band are of e_g type; the π-like interactions with oxygen p states are not possible. Thus, the contrasting anomalies in dynamical charges of Y and W *may be* associated with reverse ordering of e_g and t_{2g} states in the octahedral and tetrahedral coordinations.

To simulate thermal properties of $Y_2W_3O_{12}$, we use free energy minimization (FEM) method as implemented in GULP (general utility lattice program) computer code.[21] The FEM method has been successfully used in studying thermal expansion behavior of $AlPO_4$, showing that the NTE is related to transverse thermal vibrations perpendicular to Al-O-P linkages.[22] It has also been used in the context of ZrW_2O_8,[23] obtaining insights into modes responsible for its NTE.

In the FEM method, Helmholtz free energy is obtained within a quasiharmonic approximation and using interatomic potentials which include the Coulomb energy and short-range two- and three-body potentials. FEM also uses zero static internal stress approximation (ZSISA), in which the dependency of vibrational part of the free energy on internal coordinates is ignored. Up to room temperature, most of the internal structural parameters of $Y_2W_3O_{12}$ do not change significantly[12] and ZSISA is expected to give small errors. Errors associated with the quasiharmonic approximation become important at higher temperatures. Structural parameters are allowed to change until a minimum free energy is obtained, and this process is repeated at various temperatures to obtain thermal expansion.

TABLE II. Potential parameters used for two-body Buckingham potential as seen in Eq. (1).

Potential parameters	O-O	Y-O	W-O	Unit
A	450833.3	143417.5	3307.5	eV
ρ	0.188	0.1726	0.245869	Å

We used two-body potentials with Buckingham form

$$V = \frac{q_i q_j}{r_{ij}} + A e^{(r_{ij}/\rho)} - \frac{C}{r_{ij}^6}, \tag{1}$$

where r_{ij} is the distance between the atoms i and j with partial charges q_i and q_j. A, ρ, and C parametrize the short-range part of the interatomic potential. The parameters for Y-O and O-O short-range interactions were taken from the previously reported simulation work on Y_2O_3,[24] and C was set to zero.

Partial charges of 1.8 and −1.2 were used for Y and O ions (as reported in Ref. 24), respectively. Using charge neutrality, an effective charge of 3.6 was assigned to W ion. Bulk modulus of WO_3 (171.4 GPa) obtained with first-principles density functional theory calculations and its lattice constant were used in the GULP fitting program to obtain parameters A and ρ of W-O interactions.

To accurately describe the transverse vibrations of oxygens perpendicular to Y-O-W linkage and bond bending, we used a three-body potential of the following form:

$$V(\theta) = \frac{1}{2} k_2 (\theta - \theta_0)^2, \tag{2}$$

where θ is the angle between the Y-O-W interatomic vectors and k_2 is a constant. Using the parameters in two-body potentials already determined and fitting to the experimental structure (unit cell parameters and atomic positions) at RT, the rest of the parameters were determined. Parameters used in this work are summarized in Tables II and III.

We carried out GULP-based FEM simulations in a temperature range from 10 to 300 K, obtaining the lattice pa-

TABLE III. Three-body potential parameters obtained by fitting.

A-O-M linkage	k_2	θ_0
Y1-O6-W2	0.481844	148.45
Y1-O3-W2	0.502538	156.40
Y1-O1-W2	0.501182	155.03
Y1-O5-W2	0.486561	172.40
Y2-O2-W1	0.501276	167.18
Y2-O4-W1	0.499497	157.13

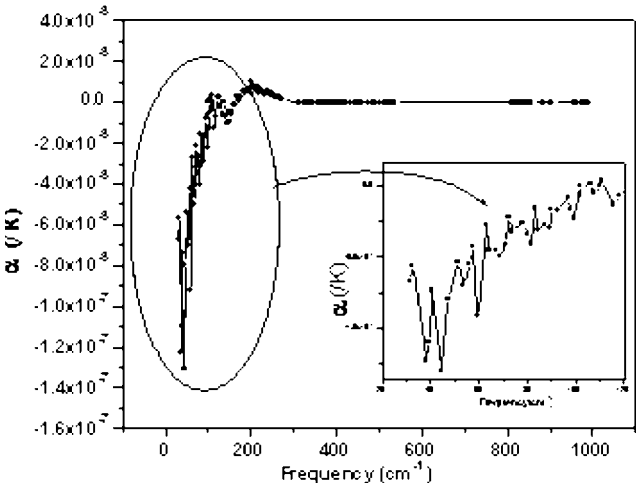

FIG. 1. Plot of α vs phonon frequency (cm^{-1}) at 250 K.

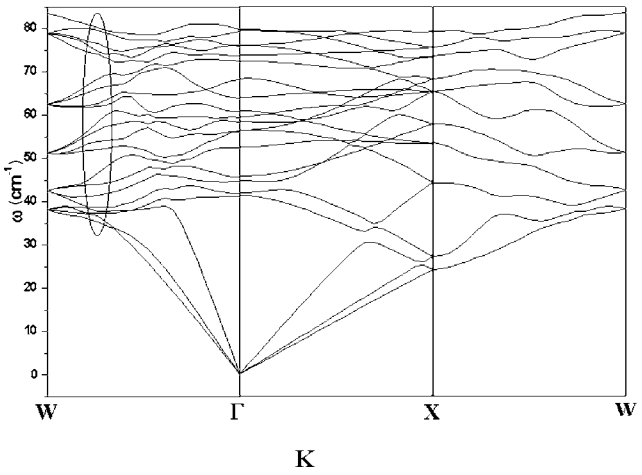

FIG. 2. Phonon dispersion relation of $Y_2W_3O_{12}$ along different k vectors where W-gamma-X represent [111], [000], and [100] vectors, respectively.

rameters, phonon modes, and frequencies at intermediate temperature. The cell parameters obtained at 10 K are $a=10.183$ Å, $b=13.892$ Å, and $c=9.926$ Å and these values agree well with experimentally observed values.[12] The unit cell volume of $Y_2W_3O_{12}$ shows contraction linearly with T, as the temperature is increased from 10 to 300 K. Our estimate of the volume thermal expansion coefficient from these results is about -3.0×10^{-6}/K.

The thermal expansion coefficient can be written as[1]

$$\alpha=\sum_i \frac{\gamma_i c_i}{3B}, \tag{3}$$

where $\gamma_i=-\frac{\partial \ln \omega_i}{\partial \ln V}$ is the Gruneisen parameter, ω_i being the frequency of mode i, c_i is its contribution to the specific heat, and B is the bulk modulus. The thermal expansion coefficient can be rewritten as

$$\alpha=\frac{1}{3B}\sum_i \frac{V\partial\omega_i}{\omega_i\partial V}\left(\frac{\hbar\omega_i}{k_BT}\right)^2\frac{e^{\hbar\omega_i/k_BT}}{(e^{\hbar\omega_i/k_BT}-1)^2}. \tag{4}$$

We now proceed to determine mode-by-mode contribution to the NTE at $T=250$ K. For the equilibrium volume V, and volumes $V+\Delta V$ and $V-\Delta V$, where $\Delta V=0.01$ V obtained with isotropically changing the unit cell parameters, we determined phonon frequencies. Using a finite difference formula for derivatives, we obtain

$$\frac{\partial\omega_i}{\partial V}\approx\frac{\omega_i(V+\Delta V)-\omega_i(V-\Delta VV)}{2\Delta V}.$$

Using this and Eq. (4), and summing over all phonons with Bloch vectors on a $2\times2\times2$ uniform mesh in the Brillouin zone, our estimate of the linear thermal expansion coefficient at 250 K is -1×10^{-6}/K, consistent with that obtained from the above results for volume versus temperature. We find [see Fig. 1 (inset)] that the phonon modes with frequencies less than 80 cm^{-1} (10 meV) are the major contributors to the negative thermal expansion. These phonon frequencies are slightly higher in energy compared to that in ZrW_2O_8 which is of the order of 3 meV. It is also evident from Fig. 1 that there is cancellation among contributions from different modes to α.

Errors in computational determination of very low-energy phonons can be sizable (even in density functional theory based calculations). This and the fact that there is cancellation among negative and positive contributions to α from low- and high-energy phonons, respectively, make determination of α quite challenging. Our estimate of α is not in good agreement with experiment,[12] and it is largely due to (a) use of a simple classical potential and (b) the quasiharmonic approximation used here. Similar discrepancies have been noticed in other calculations of α for other materials.[25] These errors should not change our conclusions about identification of the modes responsible for NTE.

Phonon dispersion of $Y_2W_3O_{12}$ from GULP calculations at 250 K is shown in Fig. 2, focusing on the low-energy phonon modes that contribute predominantly to NTE. Phonons with frequencies of about 50 cm^{-1} exhibit overlap or mixing between acoustic and optic modes near the W point (encircled region in Fig. 2). These are the phonons which contribute most significantly to negative thermal expansion, as seen in Fig. 1.

We now visualize the atomic displacements corresponding to these phonons (see Fig. 3). A phonon mode at 77 cm^{-1} [Fig. 3(a)] exhibits transverse thermal vibrations of O perpendicular to the linkage between polyhedra. The displacements of oxygens are greater than those of Y and W. It enables a back and forth rocking motion of polyhedra which can be a cause of the NTE. As a result of this motion, neighboring polyhedra rotate in clockwise and anticlockwise directions in a cooperative fashion such that the framework buckles internally. This low-energy vibrational mode is a characteristic of the framework-type crystal structure; hence, the NTE associated with it is structural in origin.

Another vibrational mode, with a frequency of 38 cm^{-1} [Fig. 3(b)], also contributes significantly to NTE. This phonon mode shows significant displacement of Y and W atoms, in contrast to the previous vibrational mode, with small displacements of oxygen atoms. It appears to have a transla-

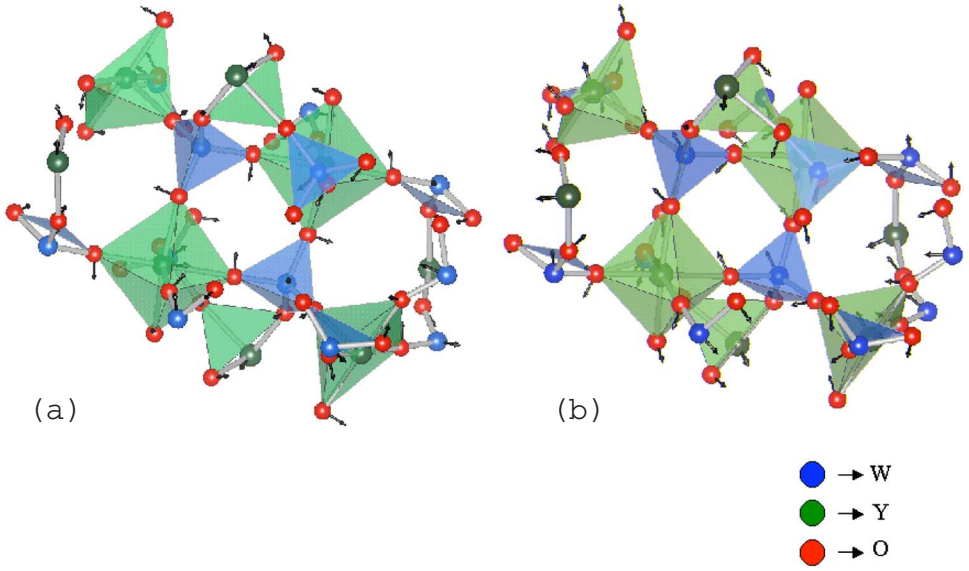

FIG. 3. (Color online) Atomic displacements corresponding to phonon modes of frequencies (a) 77 cm^{-1} and (b) 38 cm^{-1}, which contribute significantly to the negative thermal expansion of $Y_2W_3O_{12}$. Length of arrows is proportional to atomic displacements.

tional component and be of a mixed character of acoustic and optic modes (as is highlighted in Fig. 2). Frequency of this mode was found to depend strongly on temperature (it softens with T). Generally, we find that some of the low-energy phonon modes soften as the temperature is increased, while some others change their character with temperature, indicating mixing among each other.

The two types of modes we identified here are near W point and are *not* IR active. Interestingly, the first type of modes [Fig. 3(a)] has oxygen displacements along directions for which their Born charges are anomalously small, whereas the second type of modes [Fig. 3(b)] consists of displacements of Y, W, and O along directions for which their charges are anomalously large. In the long wavelength limit, the latter couple strongly with IR radiation, while the former do not. The NTE arising from the latter is similar, in principle, to that below the ferroelectric phase transitions.

In summary, while our estimate of α of $Y_2W_3O_{12}$ agrees only qualitatively with experiment, we have identified phonon modes that are relevant to the unusual phenomenon of NTE. Phonon modes with energy of the order 4–10 meV are found to be the major contributors to NTE with significant mixing of acoustic and optic branches. In addition to the previously reported transverse vibrational modes, we find that phonon modes with translational (acoustic) component are also major contributors. The presence and mixing between low-energy optic modes and translational (acoustic) modes seem to arise from partly covalent bonding between the transition metal atoms and oxygen, as indicated by the Born dynamical charges which are anomalously large or small.

We thank Vijay Shenoy, MRC for discussions and help with the use of GULP. One of the authors (U.V.W.) acknowledges support from the DuPont Young Faculty grant.

[1] N. W. Ashcroft and N. D. Mermin, *Solid State Physics* (Saunders College, Philadelphia, PA, 1976).
[2] T. A. Mary, J. S. O. Evans, A. W. Sleight, and T. Vogt, Science **272**, 90 (1996).
[3] A. W. Sleight, Curr. Opin. Solid State Mater. Sci. **3**, 128 (1998).
[4] A. K. A. Pryde, K. D. Hammonds, M. T. Dove, V. Heine, J. D. Gale, and M. C. Warren, J. Phys.: Condens. Matter **8**, 10973 (1996).
[5] A. P. Ramirez and G. R. Kowach, Phys. Rev. Lett. **80**, 4903 (1998).
[6] T. R. Ravindran, A. K. Arora, and T. A. Mary, Phys. Rev. Lett. **84**, 3879 (2000).
[7] G. Ernst, C. Broholm, G. R. Kowach, and A. P. Ramirez, Nature (London) **396**, 147 (1998).
[8] R. Mittal, S. L. Chaplot, H. Schober, and T. A. Mary, Phys. Rev. Lett. **86**, 4692 (2001).
[9] J. N. Hancock, C. Turpen, Z. Schlesinger, G. R. Kowach, and A. P. Ramirez, Phys. Rev. Lett. **93**, 225501 (2004).
[10] A. W. Sleight, *Solid State Chemistry of Materials IV*, MRS Symposia Proceedings Vol. 755 (Materials Research Society, Warrendale, PA, 2002), Article no. DD10.6.
[11] V. Korthius, N. Khosrovani, A. W. Sleight, N. Roberts, R. Dupree, and W. W. Warren, Jr., Chem. Mater. **7**, 412 (1995).
[12] P. M. Forster and A. W. Sleight, Int. J. Inorg. Mater. **1**, 123 (1999).
[13] J. Z. Tao and A. W. Sleight, J. Solid State Chem. **173**, 442 (2003).
[14] S. Sumithra and A. M. Umarji, Mater. Res. Bull. **40**, 167 (2005).
[15] W. Zhong, R. D. King-Smith, and D. Vanderbilt, Phys. Rev. Lett. **72**, 3618 (1994).

[16] X. Gonze *et al.*, Comput. Mater. Sci. **25**, 478 (2002); http://www.abinit.org
[17] X. Gonze, Phys. Rev. B **55**, 10337 (1997).
[18] U. V. Waghmare, N. A. Spaldin, H. C. Kandpal, and R. Seshadri, Phys. Rev. B **67**, 125111 (2003).
[19] M. Mikami, S. Nakamura, M. Itoh, K. Nakajima, and T. Shishido, Phys. Rev. B **65**, 094302 (2002).
[20] F. Detraux, Ph. Ghosez, and X. Gonze, Phys. Rev. B **56**, 983 (1997).
[21] J. D. Gale, J. Chem. Soc., Faraday Trans. **93**, 629 (1997).
[22] J. Z. Tao and A. W. Sleight, J. Phys. Chem. Solids **64**, 1473 (2003).
[23] R. Mittal and S. L. Chaplot, Phys. Rev. B **60**, 7234 (1999).
[24] A. B. Belonoshko, G. Gutierrez, R. Ahuja, and B. Johansson, Phys. Rev. B **64**, 184103 (2001).
[25] Y. K. Kwon, S. Berber, and D. Tomanek, Phys. Rev. Lett. **92**, 015901 (2004).